Development of a Calculation Method for Determining the Permissible Dimensions of the Defect 11

Baglan Togizbayeva, Aliya Zabiyeva, Kyrmyzy Balabekova, Anuar Kenesbek

Departament of Transport, transport technic and technology, Faculty of Transport and energy, Eurasian National University name of L.N. Gumilyov
Kazhymukan street 13, 010000 Astana, Republic of Kazakhstan
e-mail: togizbayeva_bb@enu.kz, zabiyeva_ab@enu.kz, balabekova_kg@enu.kz, kenesbek_ab_1@enu.kz

Abstract: This article deals with the issue of derailment of the wheels in railway transport, due to the probabilities of the wheel rolling on the rail. We proposes a method for calculating the maximum allowable sizes of defects 11, at different angles of the wheel on the rail with different shapes and sizes of wear of the wheel and rail edges. This technique allows us to calculate the permissible dimensions of Defects 11, according to the conditions of rolling the wheel crest onto the rail with the most unfavorable combination of interacting parts.

Keywords: Finite element method; rail; wear; traction; train; crack; internal longitudinal crack (ILK)

1 Introduction

According to statistics, the reason for the largest part of the rolling surface defects of rails in Kazakhstan is metal shelling because the contact fatigue strength of the metal is not enough (defects 11.1-2) [1]. They are formed in the working part of the rail head when the metal under the influence of alternating train loads works in a zone of limited endurance. After skipping a certain tonnage, in places where there are non-metallic inclusions in the head, lying at a depth of 3-15 mm, there are dents and so-called «dark spots», indicating the presence of an internal longitudinal crack (ILC) in the rail head. According to the instructions [2], rails with a depth of more than 3 mm and «dark spots» with a load capacity of more than 10 million tons of gross km per year should be replaced as planned. However, with the sharp increase in the cost of materials for the upper structure of the track characteristic of modern conditions, the absence of a required contingent of track fitters and the limitation of issued «windows», there are sections of track on the road network on which up to

20% of rails have defects 11.1-2 and they are replaced with a continuous change of rails or during major repairs of the track. In agreement with planned procedure, according to the results of inspections of the track, only 5-6% of rails with defects 11.1-2 are removed. Therefore, a sufficiently large number of rails with contact fatigue shelling are working on the way.

The defects 11 formed on the working surface of the rails can be conditionally divided into several groups with differences in the signs of the depth of occurrence and the form of manifestation, which in turn affects the further operation of rails with these defects. The first group includes surface defects in the form of a grid of small cracks and small stains up to 3 mm deep, the "peeling" or "fish scales", which can spread throughout the entire rail. These stains do not affect the strength of the rail, but they interfere with the control of rails by standard means of track flaw detection, which significantly complicates the identification of other defects of the rail head. This reduces traffic safety and in some cases forces decisions on early replacement of rails. The second group includes dark and light spots on the side working edge of the rail and often accompanying metal splashes. These spots are formed above the internal longitudinal crack, which lies at a depth of, as a rule, 3-8 mm, and leads to the staining of the metal surface during further operation. The danger of these defects is explained by the fact that the zone of development of transverse fatigue cracks (defect 21.1-2) coincides with the zone of development of the internal longitudinal crack, i.e., the transverse crack develops in the line inclusion of alumina, which is the focus of the internal longitudinal crack. Since the longitudinal crack passes over the transverse one, it is difficult and most often impossible to determine the internal longitudinal crack by means of track flaw detection. However, after the split of the melted metal, the conditions of interaction of the "wheel-rail" system change and the absence of contact of the wheel with the lateral working edge of the rail at the point of the breakout excludes any further development of a transverse crack. The third group includes damage to the rails in the form of gouges on the side of the working face. Depending on the operating conditions and the depth of occurrence of non-metallic inclusions, they can be shallow (up to 4 mm) and small in length (up to 10 mm), arranged either singly or several pieces in a row, or of more significant dimensions (depth up to 14 mm, length up to 300 mm, and also possibly the merger of several dents), which, with the tightening of operating conditions and the general deterioration of the condition of the path, are becoming more common [4].

Of particular importance are the studies of the strength of rails with the shape of defects 11. This is due to the fact that when large sizes are reached in the cross section of the notch, the strength properties of the rail weaken. It is considered that when the cross-sectional area is reduced by more than 30%, it is necessary to replace the rail. Thus, it can be assumed that with certain sizes of gouges, there is a danger of breaking the rails under the train, and therefore such rails must be transferred to the category of acute defects. In addition, significant geometric dimensions in length and depth do not only worsen the local dynamic impact, but also significantly increase the likelihood of rolling the wheel crest onto the rail.

In this regard, the question arises of determining the criteria by which the replacement of rails with defects 11 should be carried out and the establishment of their boundary dimensions at which the operation of rails is safe.

Analysis of a huge number of rails being removed from the track due to various defects, rail breaks under trains, accidents and wrecks shows the presence of errors in the operation of flaw detection tools, the lack of reliable methods for predicting the survivability of rails and assessing their service life. Therefore, an important area of research on the fatigue strength of rails is undoubtedly the development of methods that allow predicting the service life of rails in transit.

2 Hypothesis and Methods

Methods should be based both on the processing of statistical data of the analysis of defects in rails and the construction on this basis of the function of the probable distribution of possible defects, and on the analysis of fatigue stresses and deformations to predict the durability of rails. These methods, as a rule, provide a good match of the calculated data with the operational ones.

Promising studies in the field of the rail problem are [3] [4]:

- Investigation of the causes of the origin and development of contact fatigue damage in rails using methods of fracture mechanics
- Further study of the effectiveness of grinding rails to remove nascent cracks on the rolling surface and reduce contact stresses
- Development of mathematical models of the mechanism of formation of contact-fatigue defects taking into account the volumetric deformation characteristics of rail steel
- Conducting comparative tests in operational conditions of rails restored by surfacing

A successful solution to the problem of ensuring the safety of train traffic on rails with defects 11 is unthinkable without a full study of the strength characteristics of rail steel.

To assess the structural strength of rail steel, it is necessary to take into account the properties that characterize the strength of steel under the conditions of the stress state that exists in the rail head experiencing the greatest specific pressures from the contact application of the load. To characterize the statistical strength, these properties must be determined at a static load position: for fatigue strength, at a long cyclic contact stress. At the same time, it is advisable to use strength parameters to assess the structural strength of steel, which could be used to calculate the load strength of the rail.

Some issues of the strength of rails with cracks are considered in [6] [8] [9].

The static bending strength of rails is characterized by two parameters: the load at which a residual deformation appears, and the load at which the rail is destroyed. At the same time, parameters such as the bending boom and the work of destruction are measured and calculated. The tests are carried out by applying a load to the middle of the span of the rail mounted on the supports. In, an analysis of the influence of the depth of the gouges formed on the rails of three metallurgical plants on the relative values of the fracture work, load and deflection boom during static bending of the rail is carried out. The depth of defects 11 ranged from 3 to 10 mm. The test results showed that with an increase in the depth of the gouges in this interval, the energy intensity, power intensity and plasticity decrease, and the energy intensity and plasticity decrease more (by a maximum of 90-95%) than the power intensity (by a maximum of 40-45%), but in no case, even with a depth of gouges equal to 10 mm, the level of characteristics was not achieved, in which brittle destruction of rails occurs. The length of the gouges practically did not affect the characteristics of the damaged rails.

The rapid increase in the force action from the wheels of the rolling stock on a particular section sharply raises the contact stresses and should be taken into account when assessing the level of the latter in the rails. However, in some cases, the dynamic impact of the wheel on the rail may threaten traffic safety due to a very dangerous brittle fracture, especially if there is an acute stress concentrator on the surface of the rail, which is defect 11 and the accompanying internal longitudinal crack. Therefore, the assessment of the brittle strength of rails with dents is of great interest.

The ability of the rail to perceive single and multiple shock loads is characterized by its total energy intensity, which is evaluated during tests under conditions of impact bending loading. The rail is laid head down on two supports spaced apart at a distance of 1 m and struck in the middle of a meter span with a 1,000 kg striker raised to a certain height. The energy intensity is characterized by the magnitude of the destruction work in joules.

Changes in the brittle strength of rails with gouges from 1 to 4 mm deep were studied by Kargapoltsev S.K. [7] for non-hardened rails P65. Studies have shown that at a temperature of -20°C, the brittle strength of rails decreases from 60-20 kJ to 10-15 kJ and does not depend much on the depth of the gouges. The presence of defects 11 with a depth of 1-2 mm reduced the copra strength at the same temperature of the bulk-heated rails by 6-11 times from 60 (P50) and 160 kJ (P65) to 8 (P50) and 15-25 (P65) kJ.

The next criterion for the structural strength of rails is flexural fatigue strength. Tests of rails under bending-cyclic loading are closest to the conditions of their operation on the way. Due to the fact that on the way the rail head is subject to an alternating cycle of stresses and tensile stresses in this case are the most dangerous, currently the method of testing rails under bending cyclic loading with the location of rail samples head down in the stretching zone is generally accepted. A pulsating

bending load is applied to a rail laid head down on supports located at a distance of 1 m from each other in the middle of the span with a cycle asymmetry of 0.1. A measure of the assessment of flexural fatigue strength is a limited endurance limit or the maximum load that the rail can withstand without destruction up to a given number ($2 \cdot 10^6$) cycles of its application.

Also, for rails with contact-fatigue defects, survivability is determined, i.e., the number of loading cycles from the beginning of the formation of a fatigue crack before the rail breaks brittle from this crack. 100,000 loading cycles are accepted as the norm of survivability for bulk-loaded rails. It is believed that during this time, the path between the two aisles of the flaw detector car is safely operated [10].

So, in the field of studying the structural strength and survivability of rails with defect 11, questions on the effect of gouges with a depth of more than 4 mm on the brittle strength and cold breakage of non-thermally strengthened and hardened rails have remained unexplored. The effect of gouges on the fatigue strength and survivability of rails is practically not covered. Only after considering these issues, it is possible to establish criteria that determine the safe movement of trains on rails with a defect 11.

2.1 Testing of Rails with Spoll under Cyclic Loading

The purpose of the tests was to determine the influence of vertical dynamic load on the survivability of rails with dents of various sizes, provided that the rail is located in the stretch zone.

For this purpose, 14 thermally hardened rails from different manufacturers were selected: Nizhnetagilsky and Azovstal, having a tonnage output from 190 to 592 million tons gross, full-profile samples with a length of 11.2 m with a defect 11 in the middle with a depth of 4 to 7 mm with a length of 60 up to 120 mm. The rails were removed from sections with a radius of 600 to 900 m with crushed stone ballast and wooden sleepers, on which rolling stock with axial loads of 270 kN was handled.

In order to determine the quality indicators of rail steel, its mechanical characteristics were studied and summarized in Table 1. It was found that the rails of all manufacturers, despite the difference in the missed tonnage, did not have a significant effect of operation on reducing the characteristics of the metal of hardened rails compared to the metal of rails in the initial state [11]. This confirms the conclusion [12] on the preservation of the service properties of the bulk metal of heavy types of rails.

The tests were carried out on a PDM-PU-200 (hydraulic pulsating machine) with a vertical pulsating load with an asymmetry coefficient of 0.1, a 1.2 m long sample with a notch in the middle was mounted on two supports with a design span of 1 m head down. The maximum load was 350 kN. The choice of such a load was due to

the fact that the endurance limit for new volume-hardened rails of the P65 type is 420-450 kN [13], and for the same rails with internal longitudinal crack – 280-320 kN. Therefore, it was decided to test the rails at a load average between the endurance limit for old-fashioned rails with a defect and new ones. The tests were carried out until the complete destruction of full-profile samples. The mechanical properties of the rails during the tensile and impact bending test must comply with the standards specified in Table 1, where $\sigma_н$-temporary resistance, σ_t- yield strength, $б_1$-relative elongation, ψ_1- relative narrowing, $a_н^{-40^0}$-impact strength.

Table 1

Mechanical characteristics of steel rails of type P65

Average operating of million tons gross	Cross sections	Mechanical characteristics					
		$\sigma_н$, MPa	σ_t, MPa	$б_1$, %	ψ_1, %	$a_н^{-40^0}$ mJ/ m^2	hardness, HB
266	1	1340	1046	12	32	0.22	366
	2	1332	991	13	32	0.22	363
	3	1283	976	15	35	0.22	342
	4	1259	992	18	37	0.20	339
342	1	1388	1027	13	33	0.20	360
	2	1330	980	14	32	0.19	358
	3	1284	972	14	34	0.20	340
	4	1240	986	17	38	0.20	345
422	1	1315	990	14	35	0.19	368
	2	1326	967	15	37	0.20	376
	3	1283	980	15	32	0.20	358
	4	1240	986	16	35	0.21	340

The results of the experiment are shown in Table 2.

Table 2

Characteristics of samples of thermally hardened rails of type P65 with defects 11 and the results of cyclic tests

Sample number	Missed tonnage, million tons gross	Type of heat treatment	Defect size: depth/length, mm
1	190	Hardened	6/90
2	228		6/100
3	366		6/80
4	198		7/100
5	282		6/70
6	329		4/120
7	366		4/70
8	392		6/100

9	213		6/100
10	359		7/100
11	230		6/100
12	276		5/80
13	590		7/60
14	592		6/70

Analysis of the test results makes it possible to conclude that rails with gouges from 4 to 7 mm deep have sufficient survivability.

All samples, tonnage and type of heat treatment, have withstood the standard number of cycles to complete destruction, allowing them to be operated safely on the way.

Moreover, samples № 2, 7, 10, 11, 12 from Table 2 showed results 10-15 times higher than the standard. There was no direct correlation between the geometric dimensions of defects 11 and the survivability of rails. For example, sample No. 10 with a depth of a chink of 7 mm withstood 1178900 loading cycles before destruction, and sample No. 7 with a smaller defect depth (4 mm) accumulated 507700 cycles. The tests have shown that in the presence of a stress concentrator, such as a chink, the missed tonnage within the normative does not affect the survivability of the rails.

The study of the destroyed samples showed that the vast majority of fractures do not begin from the place of application of the load in the middle of the sample, where the dents had the greatest depth, but from the zones of the ends of the internal longitudinal crack located beyond the edges of the defect or from the edges of the dents themselves.

This indicates that microcracks present in the internal longitudinal crack propagation zone, as well as places of sharp changes in the geometry of the rail surface, are stress concentrators and additional studies of the stress state at these points are required.

The conducted studies reveal the picture of the stressed state of the metal of the rail head in the defect zone 11, the conditions of the transition of the internal longitudinal crack into the notch, show that with deep occurrence of longitudinal cracks, the cracks can reach significant sizes. If there is a geometric unevenness on the side face of the rail, which are dents, the probability of rolling the wheel onto the rail increases. It is necessary to calculate the trajectory of the wheel when rolling it onto the rail to determine the maximum permissible sizes of defects.

2.2 Calculating the Value of the Maximum Allowable Sizes of Defects 11

The works of H. Heyman [13] [14], F. Birman, [15] are devoted to the issues of wheel stability and improvement of the theory of calculations of wheel creeping onto the rail.

The conditions of the ultimate equilibrium of the wheelset are fulfilled at the moment when the left wheel on the rail is slightly raised and rests on it with its crest [17] [18]. The following forces and moments will be external to the rail threads:

1) Full dynamic vertical load P_1 transmitted at point D from the left wheel to rail A
2) The full dynamic load P_2 transmitted at the same moment from the right wheel to rail B
3) The moment M_1 acting on rail A; this moment arises due to part of P_1^P the dynamic force P_1 is applied to the neck of the axis, $M_1 = P_1^P a_1$
4) The same moment M_2 transmitted to rail B ; $M_2 = P_1^P a_2$
5) The dynamic frame force Y_p applied at a distance e from the point of contact of the left wheel with rail A. In this case, it is usually assumed that e is equal to $r_w + r_n$, where r_w is the radius of the wheel; r_n is the radius of the axis neck

The reactions of the rail threads are indicated; N_1 is the reaction of rail A normal to the U-U plane; N_2 is the vertical reaction of rail B; F_1 is the component of the tangential reaction of rail A acting in the U-U plane and assumed to be equal to $f_1 N_1$, where f_1 is the coefficient of friction of sliding the wheel crest along rail A in the plane U-U. The component of this reaction acting in the plane of the drawing, $F_1 = f_1 N_1 \cos\gamma_1$; F_1 is the component of the tangential reaction of rail B, assumed to be equal to $f_2 N_2$, where f_2 is the coefficient of friction of sliding the wheel along rail B. The component of this reaction acting in the plane of the drawing, $F_2 = f_2 N_2 \cos\gamma_2$.[10].

The friction forces $f_1 N_1$ and $f_2 N_2$ act in the opposite directions of sliding of the respective wheels. In the absence of longitudinal components of these slides, the angles γ_1 and γ_2 of the sliding direction with the longitudinal axis of the corresponding rigid base are zero; the larger these components, the larger the angles. In this calculation, the taper of the wheels is neglected (Figure 2).

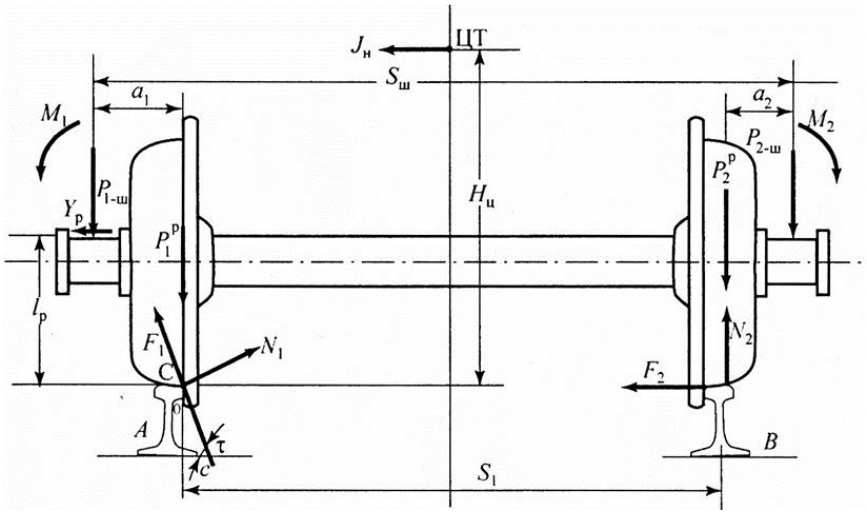

Figure 2
Diagram of forces acting on the wheel

Let us consider the conditions of the ultimate equilibrium of the wheelset at the moment when the wheel rests at point D on rail A with the rectilinear part of the ridge and tends to go down. Let's make up the equilibrium conditions of the wheelset in the form of projection equations on the U-U axis and on the axis perpendicular to it, and the equations of moments relative to the point D [10]:

$$\begin{aligned} &\text{a)} \quad (P_1 + P_2 - N_2)\sin\tau = F + \left(Y_p + F_2\right)\cos\tau \\ &b) \quad (P_1 + P_2 - N_2)\cos\tau + \left(Y_p + F_2\right)\sin\tau = N_1 \\ &\text{c)} \quad M_1 + Y_p e = (P_2 - N_2)S_1 + M_2 + F_2 h_2 \end{aligned} \tag{1}$$

The shoulder of force F_2 relative to point O is designated h_2 and is assumed positive if force F_2 passes below point D. From equation (1 c) is N_2, and from (1 b) is N_1. In order for the wheel to not roll the ridge onto the rail, the left part of equation (1 a) must be equal to or greater than the right part. The coefficient of stability against the creeping of the wheel crest on the rail

$$K = \frac{(P_1+P_2-N_2)\sin\tau}{F_1+(Y_1+F_2)\cos\tau} \tag{2}$$

At $K \geq 1$ there will be no rolling. It can be seen from equation (2) that by reducing the force f_1 or, other things being equal, the coefficient of friction f1, the coefficient of stability K can be significantly increased.

Therefore, lubrication of wheel ridges and side faces of rail heads (lubrication) is useful not only to reduce lateral wear of rails and wheel ridges, but also to increase traffic safety. Note once again that the values of P_1, P_2 and Y_p should be taken dynamically, the most unfavorable, but in really possible combinations.

When determining the stability coefficient K from equations (1b, c), the values of forces N_1 and N_2 were found, from equation (1 a) – the coefficient K.

To determine the possibility of rolling the wheel onto the rail, it is necessary to compare the vertical forces transmitted to the wheelset by the superstructure of the carriage and the frame force [109]. The safety condition under which the sliding of the wheel crest down is ensured will be the force ratio $H/Q \leq A$:

$$A = \frac{MB_1-(S_0-b_1)tg(\beta-\phi)}{S_0-(r_ш-r)[tg(\beta-\phi)+\mu} - \frac{Q_2^+[\mu b_2(S_0-b_2)tg(\beta-\phi) \quad]}{Q_1^+\{S_0-(r_ш-r)[tg(\beta+\phi+\mu) \quad] \quad \}} - \\ - \frac{S_0\{J_2\mu-J_1tg(\beta-\mu)+0.5 \quad \}mg[r-tg(\beta-\phi) \quad]}{Q_1\{(S_0-r_ш+r)[tg(\beta-\phi)+\mu \quad]\}}, \tag{3}$$

Where,

m - The mass of the wheelset

J_1 and J_2 - Vertical inertia forces of the wheelset

S_0 - The distance between the rolling circle of the wheels of the wheelset

β - The angle formed by the crest of the wheel and the horizontal plane

b_1 and b_2 - The distance from the point of contact of the rolling wheel to the points of application of forces Q_1^+ and Q_2^+

μ - Coefficient of sliding friction

$\phi = arctg\mu$

Then the ratio $\frac{H}{Q} \div A = \eta$ will be the margin of stability at the entrance of the wheel to the rail.

To ensure traffic safety, it is necessary that the value of η be greater than 1. However, even if η is less than 1, it should not be concluded from this that a wheel derailment is inevitable. Not only the necessary, but also sufficient conditions must be met for the wheel to depart. During time t, the wheel should not shift by the value of the b_{ad}. If this condition is met, there will be a convergence. Depending on the length and depth of the gouge, the time of rolling the wheel onto the rail will be reduced and, consequently, the probability of a derailment will increase. Condition $y \leq b_{ad}$ is a sufficient condition to ensure traffic safety. In order to determine the cross-section of the wheel relative to the side surface of the rail, it is necessary to make a condition taking into account the components caused by rolling dw_y and sliding du_y [10].

$$dy = dw_y + du_y \tag{4}$$

Assuming that:

$$dt = \frac{1}{v} dx$$

where,

v – the constant speed of the wheel, we get:

$$Y^1 = w_y^1 + u_y^1$$

The value of u_y and the expression (4) is the relative transverse sliding of the wheel

$$U_y = \frac{1}{v} \frac{dU_y}{dt}. \quad (5)$$

Differentiating (4) by x we get

$$Y^{11} = u_y^{11} + w_y^{11} \quad (6)$$

The curvature of the trajectory traversed by the wheel during rolling is determined by the equality:

$$Y^{11} = \lambda^2 y + \psi^1 - d_0 \quad (7)$$

Where,

$\psi = \frac{1}{v} \frac{d\psi}{dt}$ – the relative angular slip

ψ – the angle of rotation of the wheel during angular sliding

λ and d_0 – variables determined by the relations

$$\lambda = \sqrt{\frac{tg\alpha + tg\beta}{2S_1 r}} \quad (8)$$

$$d_0 = \frac{h - y_0 tg\beta}{2S_1 r} \quad (9)$$

where,

α and β	are the angles formed by the banding part and the crest of the wheels in the horizontal plane
S_1	distance between wheelset circles
γ	the radius of the wheel in the riding circle
h_0	the amount of lifting of the oncoming wheel at the initial moment of contact of the ridge and the rail, counted from the position when both wheels touch the rails on the average riding circles
g_0	the transverse displacement of the wheel from the point of contact of the middle circle of the wheel with the rail before the onset of the ridge

Substituting (8) into (7), we get:

$$y^{11} = U_n^{11} - \lambda^2 y + \psi^1 - d_0. \quad (10)$$

Denoting f(x)= $U_y^{II} = \psi^I - d_0$ we obtain the following inhomogeneous differential equation that determines the trajectory of the wheelset when the wheel crest is rolled onto the head of a flat rail:

$y^{11} + \lambda^2 y = f_0(x)$ (11)

Using the Laplace transform, we move from equation (11) to the operational equation:

$p^2y - c_1p - c_2 + \lambda_2 y = F(p)$ (12)

where $y(p) \rightarrow y(x)$ $c_1 = y_0$ $c_2 = y_0^1(0)$

$y(p^2 + \lambda^2) - (c_1p - c_2) = F(p)$ (13)

$u_y = \frac{F(P)}{p^2+\lambda^2} + \frac{c_1p+c_2}{p^2+\lambda^2}$, (14)

where $F(P)$ – function image $f(x)$, $F(P) \rightarrow F(x)$

$\frac{a}{p^2+a^2} = \sin\lambda t$ (15)

$\frac{p}{p^2+a^2} = \cos\lambda t$ (16)

We apply the folding formula:

$F_1(P)F_2(P) \rightarrow f(q)f_2(1-q)dq$ (17)

considering that:

$Y = \frac{1}{p^2+\lambda^2}F(p) + \frac{c_1p}{p^2+\lambda^2} + \frac{c_2}{p^2+\lambda^2}$, (18)

we get the expression:

$Y = \int_0^t f_0(q)\sin\lambda(x-q)dq + c_1\cos\lambda x + c_2\sin\lambda x$ (19)

The derivatives of the integration constants c_1 and c_2 in expression (19) can be determined based on the fact that at the moment when the wheel begins to run into the rail, the derivative of the function describing the trajectory of the wheelset is equal to the angle of approach χ_0:

$y|_{y_{x=0}} = 0 \cdot y^1|_{y_{x=0}} = \chi_0$ (20)

using (20) we get $c_1=0$, $c_2 = \frac{\chi_0}{\lambda}$. Substituting into the expression (19) we have:

$y = \frac{1}{\lambda}\left[\int_0^t f_0(q)\sin\lambda(x-q) + \chi_0\sin\lambda x\right] \leq b_{\text{доп}}$. (21)

This will be a sufficient condition that ensures that when the wheel enters the rail, there are no irregularities in the path and on the rail in the plan. If we take into account that there is a notch on one rail thread $m = m(x)$, then the initial equation (7) will have the form:

$$y^{11} + \lambda^2 y = u^{11} + \psi^1 - m^{11} - d_0 - \frac{mtg\alpha}{s_1 r} \tag{22}$$

To solve equation (22), we first determine the sliding forces caused by the forces in contact between the wheel and the rail when the wheel hits the rail. The resulting force y and *Q* will be the force:

$$P = \sqrt{y^2 + Q^2} \tag{23}$$

The angle between the direction of the force and the horizontal plane will be as follows:

$$\varphi = \text{arctg}\frac{Q}{y} \tag{24}$$

The force *P* can be decomposed into two components: the first component *N* is directed normal to the contact pad, and the second F_k is located in the plane of the contact pad, and the conditions are met for these forces:

$$N = P\sin(\beta + \phi_0); F_k = P\cos(\beta + \phi_0) \tag{25}$$

In addition, for slides, you can write:

$$u \overset{x}{y} = u_k \cos\beta \tag{26}$$

As a first approximation, it can be assumed that the contact pad at the point of contact of the wheel and the rail is located in the *Q* plane passing through the *x* and *k* axes and inclined at an angle β in the horizontal plane.

The forces F_k and F_x act on the contact pad in the *Q* plane, and the forces *N* act on the normal. In the case under consideration, the longitudinal force of F_x can be neglected. Using the formulas given in [11], we determine from the known components of the tangent and normal forces relative to sliding in the direction of the *K* axis:

$$u_k = \frac{3\eta\mu N\psi}{\pi clG} \tag{27}$$

Where,

η	The parameter of relative sliding in the direction of the K axis
μ	The coefficient of friction at rest
c and *l*	Respectively, the large and small semi–axes of the contact half-ellipse
ψ	The value depending on the ratio of the semi-axes of the contact ellipse
G	The shear modulus of elasticity

ψ is defined from the following expressions:

The complete elliptic integrals for $|k| \leq 1$ will have the form:

$$\left.\begin{aligned} B &= \int_0^{\pi/2} \frac{\cos^2\theta d\theta}{(1-k^x\cos\theta)^{1/2}} \\ C &= \int_0^{\pi/2} \frac{\sin^2\theta\cos^2\theta d\theta}{(1-k^x\cos^2\theta)^{1/2}} \\ D &= \int_0^{\pi/2} \frac{\sin^2\theta d\theta}{(1-k^x\sin\theta)^{1/2}} \end{aligned}\right\} \quad (28)$$

by

$$l \geq c \cdot k = \sqrt{1-c^2/l} \quad (29)$$

$$\psi = (D - \delta C)\frac{c}{l} \quad (30)$$

The values of ψ at different *l/c* ratios are given in Table 3.

Table 3

The value of depending on the ratio of the small and large semi-axes of the ellipse

l/c	0/075	0/1	0/2	0/3	0/6	0/8	1/0
ψ	0.956	0.980	0.955	0.891	0.830	0.747	0.727

To determine the values of the semi-axes of the contact ellipse, one can use the Hertz theory [8]. The minor semi-axis of the contact ellipse is determined by the formula:

$$C = \sqrt{\frac{3(1-\delta)gL\rho N}{3\pi G}} \quad (31)$$

where G – Poisson's ratio.

$$g = \frac{c}{l} \quad (32)$$

where ρ – the characteristic of the dimensions of two elastic bodies (wheels and rails), the value of which is determined by the formula:

$$\frac{1}{\rho} = \frac{1}{4}\left(\frac{1}{R_x^+} + \frac{1}{R_x^-} + \frac{1}{R_k^+} + \frac{1}{R_k^-}\right) \quad (33)$$

Where $\frac{1}{R_x^+}$ and $\frac{1}{R_x^-}$ – the main radii of curvature of the rail at the point (x=0, K=0);

To determine the values of *g* and *L* included in the formula (31), it is necessary to first determine the value of γ:

$$\gamma = \arccos\left\{\frac{\rho}{4}\left[\left(\frac{1}{R_x^+} + \frac{1}{R_x^-}\right) - \left(\frac{1}{R_k^+} + \frac{1}{R_k^-}\right)\right]\right\} \quad (34)$$

and then we will use the data from Table 3 [6].

The magnitude of the small semi - axis of the contact ellipse can be written as:

$$C = \sqrt[3]{DN} \tag{35}$$

where

$$D = \frac{3(1-\theta)\rho L g}{2\pi G} \tag{36}$$

Substituting (25) – (35) into (26) we get:

$$U^{11} = A\left(N^{1/3}\frac{d\eta}{dx} + \frac{\eta}{3N^{2/3}} \cdot \frac{dN}{dx}\right) \tag{37}$$

$$A = \frac{3\mu\beta g\cos\beta}{\rho G D^{2/3}} \tag{38}$$

$$\eta = \tau \frac{F_k}{\sqrt{F_k^2 \quad ^2 + F_x^2}}; \; F=0, \; \eta = \tau \tag{39}$$

where τ – the value characterizing slippage, is determined from the functional relationship between the value of f and τ [8]

Knowing N and defining t and $\frac{dt}{df}$, we can find U^{11} by the formula:

$$U = AN\left(\frac{dt}{df} \cdot \frac{df}{dx} + \frac{d\tau}{dN} \cdot \frac{dN}{dx}\right) \tag{40}$$

In the case under consideration, we assume that the transverse and vertical forces have the form of a rectangular pulse with a long vibration length on the rail, having the form of a half-wave of a sine wave:

$$m = A\sin\varpi x \left(0 \le x \le \frac{\pi}{\omega}\right) \varpi = \frac{\pi}{L_B} \tag{41}$$

where,

A_1 The amplitude of the unevenness value

L_B The length of the puncture

Consider a section of track with a gouge on the rail, on which the wheel runs. Considering that $x \geq L_в$ is in, and the wheel runs at an angle of χ_0 and substituting (41) and (42) in (22), we get:

$$y = \frac{u^{11}+\chi_0}{\lambda}\sin\lambda x - \frac{d_0}{\lambda^2}(1+\cos\lambda x) + \frac{A_1\varpi^2(\varpi\sin\lambda x - \lambda\sin\varpi x)}{\lambda(\varpi^2-\lambda^2)} \text{ by } x \leq x_0 \tag{42}$$

It was noted in [11] that for ratio values ranging from 1.48 to 9.56, the stability of the wheel depends not only on the ratio of forces F_y and F_x, but also on the angle of attackχ_0 and the duration of action x_0. Thus, given the values of A_1, χ_0, the calculations of y wheel edges of 10 mm are performed. In this case A_1 is the projection of the depth of the notch H, measured at an angle of 45° to the side face of the rail head, which corresponds to the depth t. The data of the calculations χ_0- angle of atack, radian, x_0- the time of action duration,secunds, carried out on the computer are shown in Table 4.

Table 4

Acceptable values of chip on the rail depending on the angle of occurrence

χ_0, rad.	x_0, sec.						
	4	**6**	**8**	**10**	**12**	**14**	**15**
0	700	600	520	510	490	450	430
0,006	580	520	430	430	420	400	390
0,0088	530	450	420	420	400	390	380
0,01	470	420	410	400	380	370	360
0,012	420	390	380	370	330	350	330
0,016	350	340	340	340	320	320	320
0,02	320	300	290	280	270	260	230

These values of geometric dimensions are the maximum permissible at which it is possible to roll the wheel crest onto the rail. The data given in Table 4 show the law of changing the permissible dimensions of the gouges from the conditions of entering the crew into the track – the permissible dimensions of defects 11 must be set at the maximum possible angles of the wheel on the rail. In general, the greatest angle of the wheel on the rail should occur in curves of small radius. However, in case of malfunctions of rolling stock and the movement of long-composite trains "herringbone" [10], the maximum angles of the run-in may be in the band of curves or straight sections of the track. Therefore, the maximum allowable dimensions of defects 11, set at the angles of occurrence $\chi_0 = 0.02$ rad, will be determined for all sections of the path regardless of curvature. Considering the most unfavorable case of interaction of the wheel-rail system, it is necessary to establish the maximum permissible dimensions of defects 11 of the conditions for rolling the wheel crest onto the rail: a length of 25 mm at a depth of 3 mm. If these dimensions are exceeded, the rails must be replaced as planned. Immediate replacement is impractical due to high costs and the random nature of the combination of factors that lead to the wheel creeping onto the rail, depending both on the condition of the rolling stock and its load, and on the condition of the rail track.

According to the method of calculating cracks, a mathematical experiment was carried out using the Solidworks program. The main characteristics of the study were temperature and load, the results are shown below (Figure 3)

a 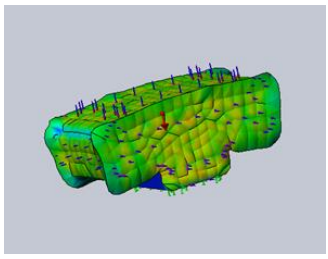 **b** 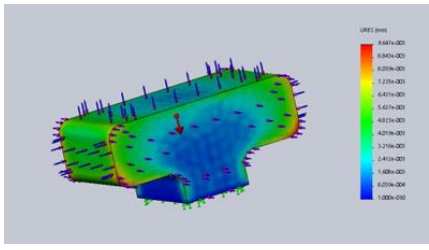

c 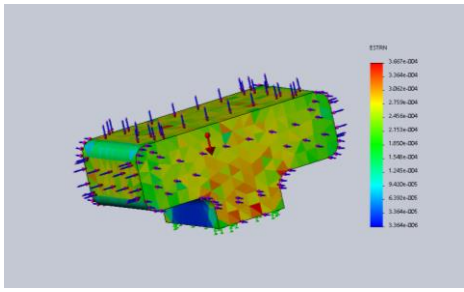

Figure 3

Impact of temperature and load on the rail depending on the depth of the crack

a- depth of the crack 1mm,b- depth of the crack 2 mm, c- depth of the crack 3 mm and more

As we can see from the analysis on lines with a sufficiently high load, where pointed rolling of wheels is more common, the probability of rolling stock derailment increases in the presence of defects 11 with a depth of more than 3 mm and a length of more than 25 mm, which proves the developed calculation methodology.

Derailment of wheels is inevitable if two conditions are met: necessary when the coefficient of stability margin at the entrance of the wheel to the rail is less than 1 and sufficient when the wheel shifts by a value bдоп equal to the projection of the wheel edge on the horizontal axis.

The determination of the transverse displacement of the wheel is reduced to the compilation of an ordinary inhomogeneous differential equation, which includes components due to rolling and sliding. This allows considering a sufficient condition that ensures traffic safety when the wheel enters the rail, which does not have defects in the riding surface.

Conclusions

In this article we described methods of calculating the value of the maximum allowable sizes of defects 11 at different angles of the wheel running into the rail with different shapes and sizes of wear of the wheel and rail edges.

The presence of a spoll on the rail raises the likelihood of the wheel rolling onto the rail. To solve the problem of the maximum allowable size of the gouges, a theoretical study of the interaction of a wheel with various wear with a rail head having a Defect 11 was carried out. The analysis used previously conducted studies [10] with the introduction of a component into the calculations in which the dents are represented as half-waves of a sine wave.

The given calculation method makes it possible to establish the permissible dimensions of Defects 11 according to the conditions of rolling the wheel crest onto the rail with the most unfavorable combination of interacting parts. On lines with a sufficiently high load, where pointed rolling of wheels is more common, the probability of rolling stock derailment increases in the presence of Defects 11 with

a depth of more than 3 mm and a length of more than 25 mm. On road sections where there is no heavy train traffic, less stringent restrictions should be set on the size of the gouges (4 mm depth and 36 mm length). The appearance of defects of 11 large sizes should serve as a reason for the appointment of a planned replacement of the rail, however, it would be more economical to repair the rail in transit.

References

[1] Wu L., Wen Z., Jin X. Finite element analysis of wheel/rail frictional temperature during wheel complete slides on rail. Jixie Gongcheng Xuebao. 2018, T. 44. № 3, pp. 57-63

[2] Zh Arystanov, B. Togizbayeva,. A. Karazhanov,. Zh. Alipbayev,. K. Burkanova Investigation of the impact of operating conditions on the service life of locomotive wheelset tyres 2022 Journal of the Balkan Tribological Association T. 28, № 6, pp 882-896

[3] Sergeev A. I., Suvorov A. A. Improving the electrical characteristics of measuring devices based on rail-to-rail operational amplifiers. Measurement Techniques. 2018, T. 61. № 8, pp. 817-823

[4] Tadić N., Zimmermann H., Zogović M., Banjević M. A low-voltage complementary metal-oxide semiconductor adapter circuit suitable for input rail-to-rail operation. International Journal of Electronics. 2019, T. 97. № 11, C. 1283-1309

[5] Królicka A., Lesiuk G., Mech R., Radwański K., Kuziak R., Janik A., Zygmunt T. Comparison of fatigue crack growth rate: pearlitic rail versus bainitic rail. International Journal of Fatigue. 2021, T. 149. p. 106280

[6] Mao X., Shen G. A design method for rail profiles based on the geometric characteristics of wheel–rail contact. Proceedings of the Institution of Mechanical Engineers, Part F: Journal of Rail and Rapid Transit. 2018, T. 232. № 5, pp. 1255-1265

[7] Kargapoltsev S. K., Davadorg B. Algoritmic base for prognosis the rail residual resource of the lateral wear of rail. Innovation and Sustainability of Modern Railway. 2019, pp. 539-542

[8] Wang K., Liu P., Zhai W., Huang Ch., Chen Z., Gao J. Wheel/rail dynamic interaction due to excitation of rail corrugation in high-speed railway. Science China Technological Sciences. 2019, T. 58. № 2, pp. 226-235

[9] Ju B., Zhu H., Wang Z., Sun Z., Xu J. Rail contour matching method based on random vibrations of a rail inspection vehicle. Zhendong yu Chongji. 2019, T. 36, № 3, p. 65-69

[10] Shiyao Lu, Jingru Wang, Guoqing Jing, Weile Qiang, Majid Movahedi Rad: Rail Defect Classification with Deep Learning Method, DOI: 10.12700/APH.19.6.2022.6.16, pp. 225-241

[11] Ren M., Dong C., Qin M., Wang B., Han X. A novel slew-boosting circuit for rail-to-rail operational amplifier. Journal of Circuits, Systems, and Computers. 2021, T. 30, № 2, p. 215

[12] Maxim Arbuzov, Serhii Tokariev, Oleksii Hubar, Volodymyr Andrieiev, Volodymyr Suslov: Relaxation of the Elastic Clamp in Rail Fastenings, DOI: 10.12700/APH.19.3.2022.3.17, pp. 219-230

[13] Ljubo Marković, Ljiljana Milić Marković, Srđan Jović, Miloš Milovančević: Evaluation of Alternative Solutions of General Design of Railway Lines with Regards to Environmental Protection, DOI: 10.12700/APH.19.6.2022.6.8, pp. 184-214

[14] Vesna Jovanovć, Dragoslav Janošević, Dragan Marinković, Nikola Petrović, Jovan Pavlović: Railway Load Analysis During the Operation of an Excavator Resting on the Railway Track, 10.12700/APH.20.1.2023.20.6, pp. 79-93

[15] Aditjandra P. T., Zunder T. H., Islam D. M. Z., Palacin R. International Series in Operations Research and Management Science. 2019, T. 226, pp. 413-454

[16] Eller, B., Fischer, S. Tutorial on the emergence of local substructure failures in the railway track structure and their renewal with existing and new methodologies (2021) *Acta Technica Jaurinensis*, 14 (1), pp. 80-103

[17] Slobodan Rosić, Dušan Stamenković, Milan Banić, Miloš Simonović, Danijela Ristić-Durrant, Cristian Ulianov: Analysis of the Safety Level of Obstacle Detection in Autonomous Railway Vehicles, DOI: 10.12700/APH.19.3.2022.3.15, pp. 187-205

[18] Dmytro Kurhan, Mykola Kurhan, Nelya Hmelevska: Development of the High-Speed Running of Trains in Ukraine for Integration with the International Railway Network, DOI: 10.12700/APH.19.3.2022.3.16, pp. 207-218